Gas slip modeling for bullheading applications

Farhan Rasheed[1], Magnus F. Ramstad[1], A. H. Rabenjafimanantsoa[1], and Kjell Kåre Fjelde[1]

Department of Energy and Petroleum,
University of Stavanger, Norway

Abstract. Bullheading is the process of pumping gas bubbles downwards in a well. Since gas tends to migrate upwards on its own, a certain critical liquid rate is required to be able to move the gas downwards. The bullheading procedure is used for killing production wells and it is also a backup well kill solution if a gas influx is taken during the drilling of new wells. It is also used in a special drilling system developed for handling large drilling fluid losses in carbonate formations. One-dimensional two-phase flow can be described by the Drift-Flux model. Here the gas slip relation is essential to predict how gas moves relative to liquid. This relation depends on two parameters. One parameter is the gas rise velocity which describes how fast a gas bubble moves relative to stagnant liquid. The other parameter, the gas distribution coefficient is more related to the shape of the gas bubble. In the literature, one will find that the models were mainly developed for co-current upward flow. However, there are a few papers that address how these parameters will change when considering co-current and downward two-phase flow. A medium size experimental arrangement has previously been built at the University of Stavanger and experimental bullheading data from the loop was compared against the results achieved from the gas slip relation and the drift flux model. When they considered a Newtonian fluid and slug flow (Taylor bubbles), large differences were seen. It was much harder to push the gas down in practice compared to what the simulation model predicted. In this paper, the experimental loop will be described along with some improvements done before repeating the experiments. It will be shown that still there was a large discrepancy between model predictions and the experimental data. Here one will also emphasize how a simulation model based on the Drift-Flux model is needed to be able to predict the downward gas velocities when using a specific slip relation. The large discrepancy led to a new investigation of what could be the cause. A deeper literature review considering an old paper from 1962 gave a hint that the gas distribution parameter can change dramatically when transitioning from co-current upward flow to counter-current and downward flow. The gas distribution parameter was then calibrated to obtain a better fit with the experimental data using both theoretical considerations and a workflow involving model simulations and comparison with the experimental data. The new value for the distribution coefficient differed significantly from other values proposed in the literature. The reason for this large discrepancy is most likely related to the non-symmetric behavior of the Taylor bubble in this experimental setup.

Literature seems to support that this kind of behavior exists and will have certain implications for the gas movement.

Keywords: Bullheading · Modeling · Experimental · Multiphase Flow.

1 Introduction

Wells are drilled and used for both producing hydrocarbons and extraction of geothermal energy. They are also used for hydrocarbon gas storage and in the future, storage of CO2 can become more common. Wells must be operated in a safe manner and different circulation techniques are available to remove unwanted gas content in a well.

Bullheading is the name of the operation where one tries to push gas bubbles downward in a well [1]. To overcome gas migration, a certain liquid flow rate is needed from above to push the gas downward. During conventional drilling, the pressure at the bottom of the well is kept above the pore pressure to avoid the influx of hydrocarbons from the rock formations. However, in some cases, gas influx takes place, and a well-controlled situation has emerged. Then this gas has to be removed from the well either by circulating it to the surface where it is handled safely or by forcing it back into the formation [2,3]. In this situation, it is a method that will be used if the other circulation methods do not work.

In recent years, more specialized drilling techniques have been developed. One of them is the pressurized mud cap drilling method [4]. This method was developed for drilling highly fractured and vugular carbonate formations where large losses of drilling fluid will occur. Here, the bullheading operation is quite standard, as gas often enters the well and must be pushed back into the fractures [5].

Bullheading is also used in the later stages of the life cycle of the well. A producing well must be killed for maintenance purposes if a sidetrack is to be made or if the well shall be permanently plugged and abandoned. A paper addressing the killing of live gas wells and modeling this process is provided in Oudeman [1].

A medium-sized experimental facility has been built at the University of Stavanger to investigate the dynamics of bullheading. This was done as part of a master thesis project [6]. In their study using water and air, they performed different bullheading experiments to check what flow rates were needed to be able to push the gas downward. Only Taylor bubbles were studied. However, when the experimental results were compared with a simulation model based on the Drift-Flux model approach using a gas slip relation taken from the literature, large discrepancies were observed. In a later thesis work [9], the discrepancy was investigated to see if it was caused by numerical errors in the simulation model, but it turned out that this was not the main cause although some improvements were suggested. Hence, it was decided to start a third master thesis project to redo the experiments and make a new comparison to investigate what could be the main explanation for the differences seen [10]. This paper will address the main findings and discuss this recently published literature.

2 Simulation model

In this section, we will first present the Drift-Flux model. Then a brief introduction to the numerical scheme will be given. The simulation results will be provided in the section where we present the experimental results. The model needed calibration to fit the data.

2.1 Drift flux model

The Drift-Flux approach can be used to model the bullheading process [11]. This is a one-dimensional model for two-phase flow which is composed of one mass conservation law for each phase combined with a mixture of momentum equations. It must be supplied with various closure laws like phase density models, friction model, and a gas slip relation. The gas slip relation is needed since there is only one mixture momentum equation and the gas slip relation describes how the gas moves relative to the liquid.

The Drift Flux model forms a set of nonlinear partial differential equations which is classified as hyperbolic in nature. This means that the model describes different waves propagating and these are the sonic waves propagating upstream and downstream and the contact discontinuity which forms the interface between the two-phase and one-phase regions [12].

Density models for water and air were adopted. The experiments took place at room conditions yielding a water density of around 1000 kg/m^3 and an air density of approximately 1.2 kg/m^3.

The friction model was adopted from Ghauri et al. [11]. It should be noted that the fluid viscosities were increased artificially to reduce the effect of sonic waves propagating in the simulation setup. These are typically generated when starting or stopping pumps. It was shown [9] that sonic waves could lead to misinterpretation of the value of the simulated gas velocity. But, by increasing the viscosities, the sonic waves were dampened faster and one omitted oscillating gas velocities during the bullheading process.

2.2 Gas slip ratio

The gas slip relation is defined by the following formula [13]:

$$v_g = Kv_{mix} + S = K(v_{sl} + v_{sg}) = K(v_l\alpha_l + v_g\alpha_g) + S \tag{1}$$

The mixture velocity v_{mix} is defined as the sum of the superficial liquid v_{sl} and superficial gas velocity v_{sg}. The superficial phase velocity is defined as the phase velocity multiplied by the phase volume fraction. Here v represents phase velocity and α is the phase volume fraction. The subscripts l and g indicate the liquid and gas phases.

The S variable is the gas rise velocity and represents how fast gas migrates upwards in a stagnant liquid. The value of the K parameter will vary depending on which type of flow pattern is present but also on the type of flow (upward co-current, counter-current, or downward flow). Downward flow will correspond to a successful bullheading operation in which the gas bubble is forced downward along with the liquid.

Different models exist for S depending on if bubble or slug flow is present. In this experimental work, slug flow or more specifically Taylor bubbles will be studied. The distribution parameter K will typically take the value 1.2 for upward co-current flow. However, less research has been performed on quantifying this value for countercurrent and downward flow. However, Hasan et al. [14] suggested K = 1.2 for countercurrent flow and 1.12 for downward flow.

The model for S when considering Taylor bubbles is given by the following formula [14]:

$$S = 0.35\sqrt{(gD(\rho_l - \rho_g)/\rho_l)} \tag{2}$$

This formula is well-known in the literature. Here g is the gravity acceleration, D is the inner diameter of a pipe, and ρ represents phase densities. Using water and air at room conditions combined with our experimental arrangement with an inner pipe diameter D = 0.0392 m, gives an S = 0.217 m/s. In the experiment, this was measured to 0.232 m/s during calibration of the experimental setup which gave relatively good agreement with theory. It was the experimental value that was used further in the simulation work.

It is possible to derive an expression for the critical bullheading rate that will keep a Taylor bubble static in the well while pumping liquid from above. One needs a rate higher than this to push the gas downward.

The outline of this formula is shown in Abdelgabir [9]. The formula can be derived from Eq. 1 by setting $v_g = 0$ and multiplying it by the area A of the pipe. This gives:

$$Q_{critical} = \left|\frac{-SA}{K}\right| \tag{3}$$

Here, we note that the expression also depends on the parameter K. Later, it will be shown that neither the value of 1.2 nor 1.12 fits very well with our experimental observations. Hence, this parameter will be subject to calibration in the simulation model.

2.3 Numerical Scheme

To solve the Drift-Flux model, an explicit scheme has been used. We have used a hybrid scheme where the Advection Upstream Splitting Method has been combined with a van Leer scheme (AUSMV). For more details on this scheme, one can consult Evje and Fjelde [15]. The slope limiter concept [16] has been used to reduce numerical diffusion to better capture the contact discontinuity between the two-phase and one-phase regions. A vertical pipe is then discretized into 50 cells before using the numerical scheme to simulate that gas first migrates upward before it is bullheaded downward.

3 Experimental Results and Model Comparison

The bullheading experiments were performed at the Multiphase Flow Laboratory at the University of Stavanger (UiS), Norway.

3.1 Experimental Procedure and Results

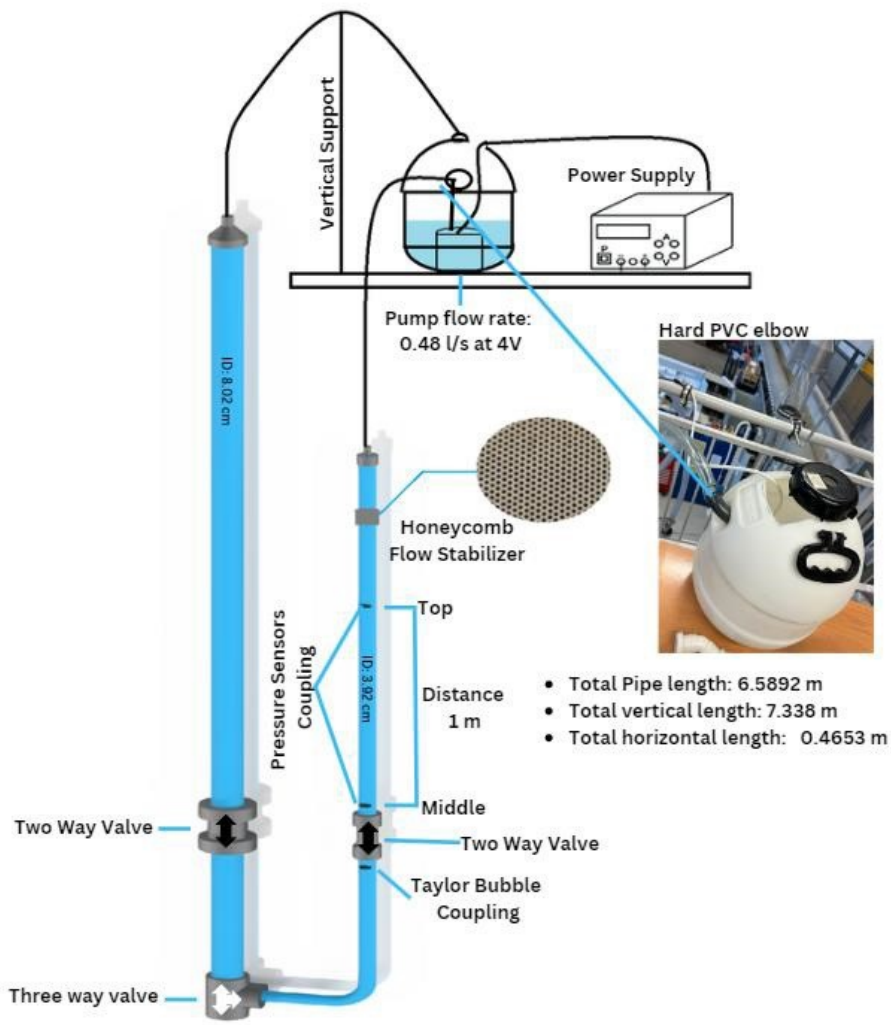

Fig. 1. The experimental setup [10].

Fig. 1 shows the present experimental setup of the bullheading experiences. This setup is the same loop as in previous experiments [6,7] but was slightly modified to ensure proper flow calibration. It consisted of two acrylic pipes mounted vertically in parallel and connected to each other from the bottom. The loop is a fully transparent U-shaped tube connected using Georg Fisher connectors, allowing for visual inspection of the whole system. The test section on the right side of the U-tube has a circular cross-section with an inner diameter of 39.2 mm and a total length of 3.685 m. At the bottom, the tubes were connected with a short pipe to direct the liquid to the left part of the pipe, which has an inner diameter of 80 mm. The flow was driven by a submersible DC voltage bilge pump (0 - 12 Volt), controlled by a power supply (output voltage/current 1-30 V/30 A), as shown in Fig. 1. The Pasco Capstone [8] dual pressure transducer PS-2181 (sample rate up to 1 kHz, 0.01 kPa resolution at 10 Hz) was used to measure the differential pressure between two pressure ports separated by 1 m apart from each other. The sensor measures differential pressure by determining the difference in pressure between port 1 and port 2. A two-way valve was mounted and kept closed before the bullheading experiments began. The volume of the Taylor bubble was controlled by displacing a sufficient amount of liquid by air from the Taylor bubble coupling, as seen in Fig. 1. A honeycomb flow straightener was inserted inside the top of the pipe to reduce disturbance in the flow and homogenize the velocity profile during bullheading experiments. This is very important to ensure an even distribution of the flow during bullheading experiments.

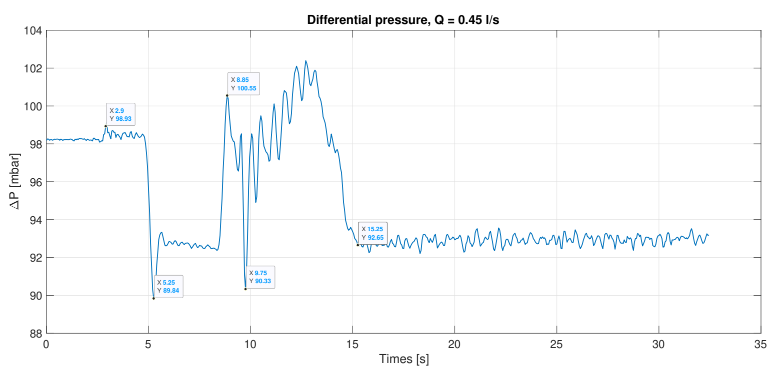

Fig. 2. Time series of the differential pressure during bullheading [10].

Before all experiments, the pump was calibrated against a Mettler Toledo balance with a fairly linear and repeatable characteristic of flow versus voltage readings. The dual pressure transducer on the other hand was calibrated using one-point calibration. To do so, an independent means of measuring barometer pressure (from Rosemount, accuracy ± 10%) was used together with hydrostatic pressure changes against water column heights.

Fig. 2 shows the time series of differential pressure during a bullheading experiment. Here, after opening the valve, the bubble is released and causes a pressure spike at 2.9s. The bubble passes the first pressure port and the second port at 5.25s and 8.85s, respectively. Between time intervals [9.75,15.25] the bubble passes both sensors, moves downward, and finally reaches a relatively constant pressure, indicating the corresponding critical rate (Q = 0.45 l/s) that is needed to keep the bubble stable.

In Fig. 3 the difference in the experimental and simulated gas velocities when K varies is presented. The data were calculated by subtracting the absolute value of the gas velocities from the experimental data with the gas velocities from the simulated data. To this end, five experimental runs were carried out and the results are presented in Table 1. More of this will be discussed in detail in the next section.

Table 1. Difference between experimental and simulated gas velocity when varying K.

Q [l/s]	0.35	0.40	0.45	0.50	0.55
Experimental Gas Velocity [m/s]	0.0542	0	-0.0490	-0.0840	-0.1242
Simulated Gas Velocity at K = 1.2 [m/s]	-0.0923	-0.1386	-0.1850	-0.2314	-0.2779
Simulated Gas Velocity at K = 1.0 [m/s]	-0.0576	-0.0989	-0.1403	-0.1817	-0.2232
Simulated Gas Velocity at K = 0.7 [m/s]	0.0290	0.0002	-0.0287	-0.0576	-0.0867

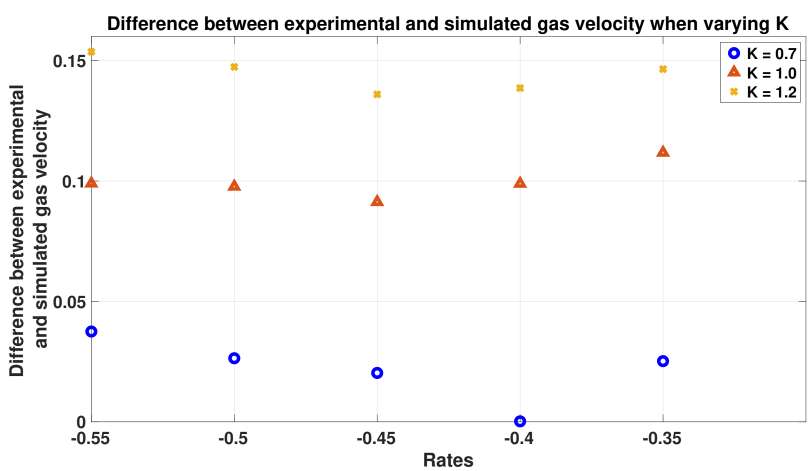

Fig. 3. Difference between experimental and simulated gas velocities when varying K [10].

During the experiments, a significant challenge was encountered when the bubble shape was asymmetric, as seen in Fig. 4. This situation made it difficult to push the bubble downward. The symmetry of the bubble broke down when bullheading because the liquid flow was greater than some critical value.

Fig. 4. Photograph of the Taylor bubble wedging during bullheading experiments [10].

3.2 Model Simulation and Calibration of Gas Distribution Parameter

The gas rise velocity S was measured to be 0.232 m/s. Using Eq. 3 with K = 1.2 the critical flowrate to keep the bubble stationary when bullheading should be 0.23 l/s. However, we saw that the critical rate observed experimentally was 0.40 l/s. The difference was quite substantial. It is more difficult to stop the gas bubble from migrating upwards than the theory predicts. This was also observed in Alarcon and Hernandez [6].

Hence, we will use Eq. 3 to calibrate the gas distribution parameter K using the observed critical rate:

$$K = \frac{AS}{Q_{criticalexp}} \tag{4}$$

The value obtained was K = 0.7 which is substantially different from K = 1.2 or K = 1.12 as reported by Hasan et al. [14].

This calibrated value should at least be valid when the bubble remains stationary. But to check how this value will fit when the Taylor bubble moves downward, for instance, use the simulation model and compare the simulated gas velocity with the gas velocity measured experimentally.

In the following, it will be shown how the simulation model was used to produce results for one of the successful bullheading experiments where the gas bubble was moved downwards.

A 3.685 meter vertical pipe was considered with an inner diameter of 0.0392 m. The S is taken from the experiment while K = 1.2 initially, since we start with a Taylor bubble moving upwards in a stagnant liquid.

A gas bubble was introduced at the bottom from 0 to 1.25 s. Then the pipe was closed on top and the gas bubble was allowed to migrate upward. Between 6.25 and 6.5 s, the bullheading rate at the top of the pipe was ramped up linearly. At the same time, the K parameter is changed to the value found from calibration (K = 0.7). We will here show the effect of using three quite different bullheading rates. Simulation will be stopped at 10 seconds and we will show the position of the gas bubble and the gas and liquid velocity. Negative velocity means that the gas is moving downwards.

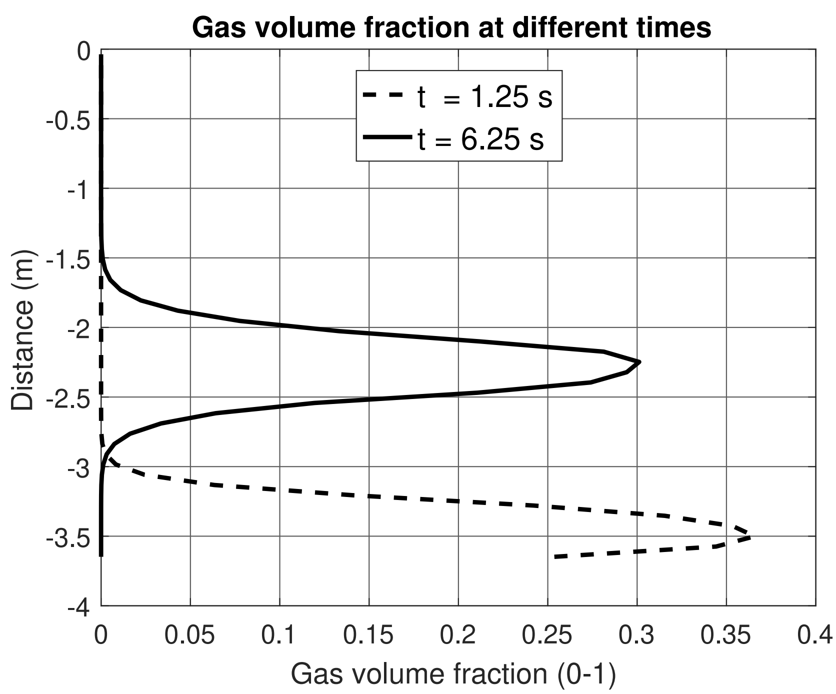

Fig. 5. Gas volume fraction at two different times during migration.

In Fig. 5, one can observe how the gas bubble migrated upwards from 1.25 to 6.25 seconds when the pipe was closed on top and no circulation took place. The simulated gas velocity at 6.25 seconds is shown in Fig. 6. It has a value equal to around 0.23 m/s and this fits well since the S parameter was set to

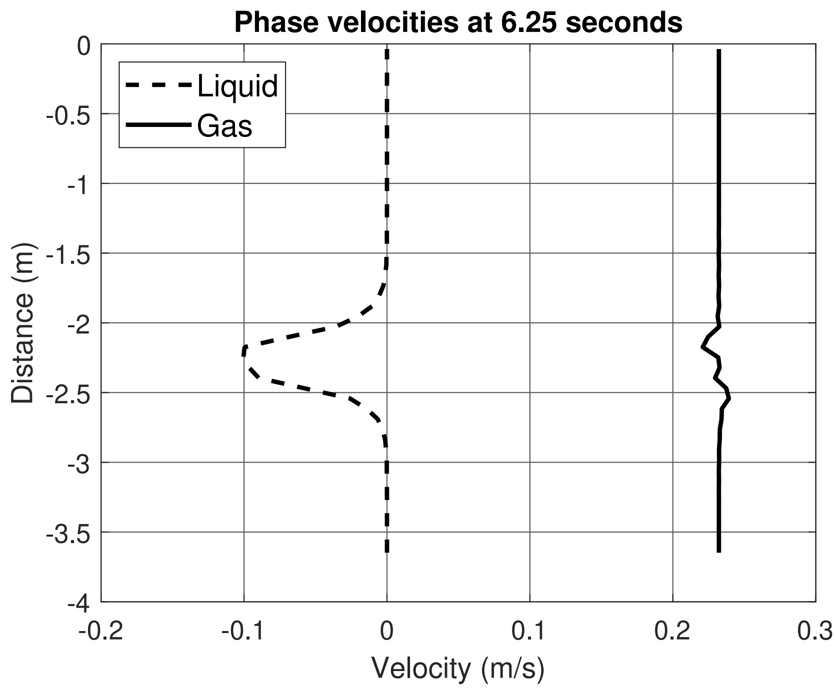

Fig. 6. Liquid and gas velocities during migration.

the value that was measured experimentally. Here, one can also observe that the liquid velocity is negative where the gas bubble is located. The liquid is flowing down on the outside of the bubble as the gas moves upward. Another observation is that both the front and the tail of the gas bubble are somewhat smeared out. This is due to numerical diffusion. The effect of numerical diffusion was shown to have no impact on the prediction of the critical bullheading rates in the numerical work performed in Abdelgadir [9]. Fig. 7 shows the situation after bullheading has been carried out for some seconds. We use three different flowrates. The black graph shows the gas volume fraction when using the critical rate observed experimentally. Comparing this to Fig. 5, we observe that the gas bubble has not moved. Fig. 8 shows that the gas velocity is zero in this case. This is what to expect since we have calibrated the gas distribution coefficient to be K=0.7. The red graph in Fig. 7 shows the situation if a bullheading rate below the critical rate is used. In this case, the gas bubble has moved even further up and Fig. 8 shows that the gas velocity is positive. The blue graph in Fig. 7 shows the situation if a bullheading rate above the critical rate is used. In this case, the gas bubble has been moved downwards and Fig. 8 shows that the gas velocity is negative. This is an example of a successful bullheading operation where the flow rate is sufficient to push the gas downwards. Fig. 9 shows the liquid velocities

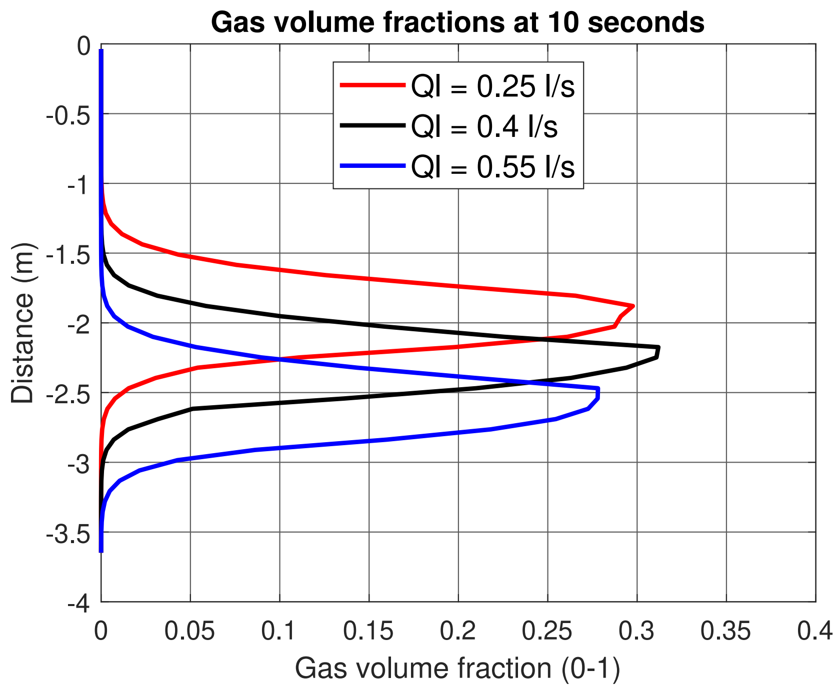

Fig. 7. Gas volume fraction at 10 seconds for three different bullheading rates.

for the different flowrates. The liquid velocity is always negative but it becomes even more negative around the gas bubbles.
As we see from this simulation example, it is possible to show what the phase velocities will be during the bullheading operation. The simulated gas velocities for various bullheading rates was then compared with the gas velocities measured experimentally.

4 Discussion

When analyzing the dynamics of Taylor bubbles, it is common to introduce dimensionless numbers to evaluate which forces and effects are the most dominating in the experiments or simulations performed. The dynamics of the flow can be influenced by inertial effects, gravity, buoyancy, viscosity and surface tension [17,18,19,21]. The Froude number expresses dimensionless velocity and is defined by:

$$v^* = \frac{v}{\sqrt{gD}} \tag{5}$$

The Eötvös number expresses the effect of gravitational forces versus interfacial forces:

$$Eo = \frac{(\rho_l - \rho_g)gD^2}{\sigma} \tag{6}$$

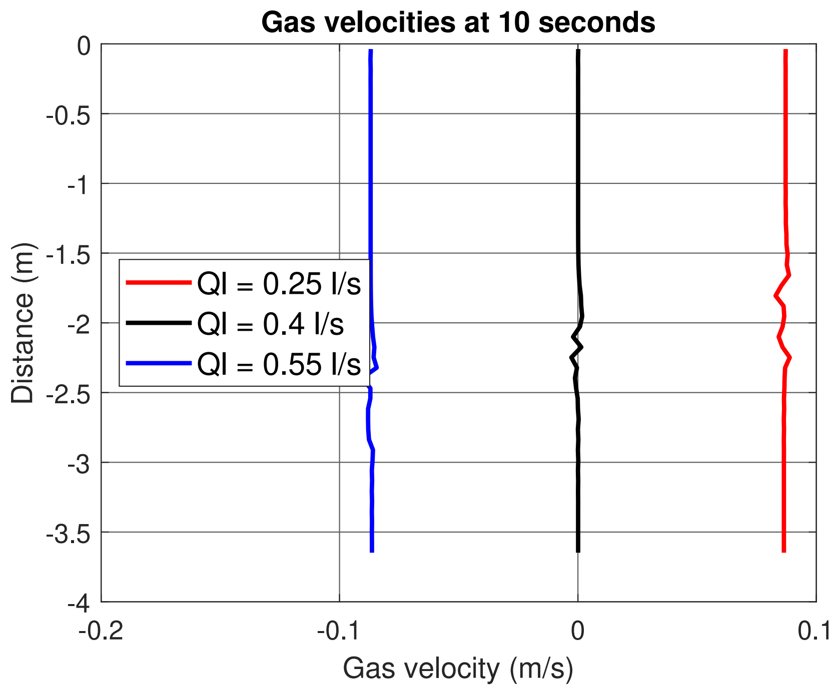

Fig. 8. Gas velocity at 10 seconds for three different bullheading rates.

Here, σ is the surface tension in N/m. A larger pipe diameter will increase Eötvös number and the effect of interfacial forces will be negligible. With reference to White and Beardmore [22], it was stated in Martin [17] that for pipe diameters less than 2 cm using air-water systems, the Eötvös number would be lower than 70 and the surface tension will start to affect on the gas rise velocity.

The Morton number expresses the ratio between viscous and interfacial forces and is expressed as:

$$Mo = \frac{(\rho_l - \rho_g) g \mu_l^4}{\rho_l^2 \sigma^3} \tag{7}$$

Here, μ_l is the liquid viscosity in Pa$\times s$. The range of the Morton number can be large and a very low number indicates a system not dependent on viscosity. In Lizarraga-Garcia et al. [19], it was reported that different oils ranging from very light oil to heavy oil were reported to give Mo $\in [5 \times 10^{-10}, 5 \times 10^3]$.

It is also common to use the inverse viscosity number N_f [20] defined as:

$$N_f = \frac{\sqrt{(\rho_l - \rho_g)\rho_l g D^3}}{\mu_l} = \left(\frac{Eo^3}{Mo}\right)^{0.25} \tag{8}$$

The inverse viscosity number will be large for a non-viscous system and vice versa.

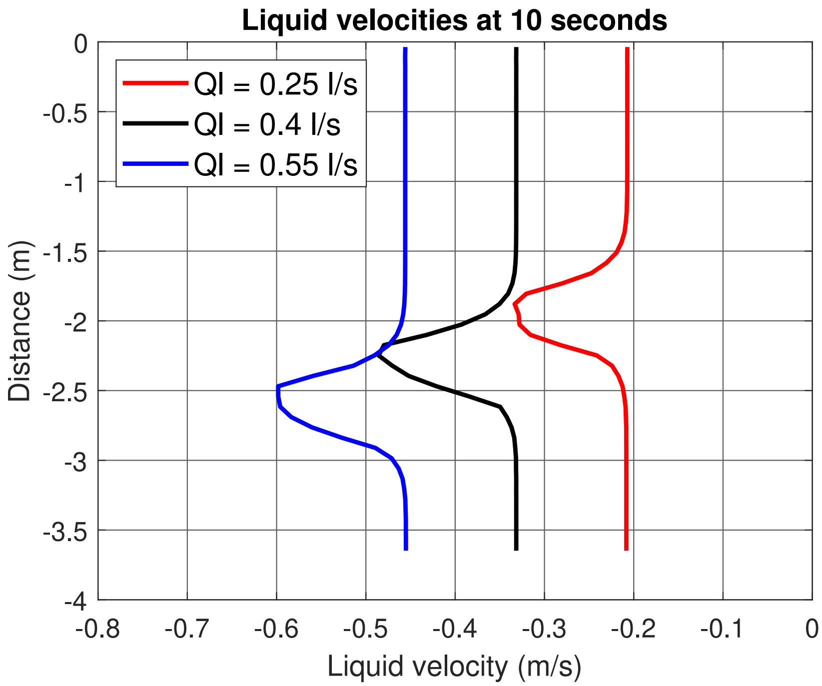

Fig. 9. Liquid velocity at 10 seconds for three different bullheading rates.

The variables in our experimental system using water and air are: D $= 0.0392$ m, $\rho_l = 1000 kg/m^3$, $\rho_g = 1.2 kg/m^3$, $\mu_l = 0.001 Pa \times s$, and it is assumed that the surface tension is: $\sigma = 0.072$ N/m. This gives us dimensionless numbers: Eo $=$ 209, Mo $= 2.63 \times 10^{-11}$ and $N_f = 24294$. As discussed in Martin [17], for Eo > 70 and $N_f > 550$, the flow is dominated by inertia and gravity. The effect of surface tension and viscosity is negligible. This can also be seen in the map provided in Lizarraga-Garcia et al. [19] with reference to White and Beardmore [22].

Historically, there has been extensive experimental research on Taylor bubbles in water-air systems. Some important references in this context are Griffith and Wallis [23], Nicklin [24], and Martin [17].

Nicklin [24] proposed a relation for the velocity of the tip of the Taylor bubble given by:

$$v_{TB} = C_0 v_l + C_1 \sqrt{gD} \tag{9}$$

Here, v_l is the average liquid velocity. He performed experiments with water and air in a pipe with a diameter of 0.0259 m and for an upward flow of liquid, C_0 was determined to be 1.2. The dimensionless gas rise velocity C_1 was 0.35 which had been discovered earlier. However, for downward liquid flow, he experienced large variations in the C_0 parameter and it was even reduced below 1. Hence, when Oudeman et al. [1] later in 1994 developed a simulation model for bullheading in gas production wells, they adopted $C_0 = 0.9$ with reference to Nicklin [24]. It should be noted that the parameters C_0 and C_1 are the same as K and S in the gas slip relation presented earlier in this paper.

The reason for the large variation of C_0 for a downward liquid flow rate was that the Taylor bubble lost its axis symmetry and became unstable. The tip of the bubble was no longer in the center of the pipe but was leaning against the pipe wall. In this situation, the bubble moved faster upwards compared to the symmetric situation leading to a reduction in C_0. This instability was observed by Griffith and Wallis [23], Nicklin [24], and Martin [17]. In Martin [17], air-water systems for 3 different pipe diameters were experimentally studied (D = 0.026 m, 0.1016 m and 0.14 m). It was seen that the Taylor bubbles became more eccentric when downward liquid rate was increased but also when the diameter increased. They reported that C_0 became 0.93, 0.9 and 0.86 for the diameters 0. 026 m, 0.1016 m and 0.14 m respectively. They also reported that C_1 increased above 0.35.

In our experiment, we calibrated K (i.e. C_1) to be 0.75. This may seem low compared to the values observed in Martin [17] but here one should keep in mind that we kept S unchanged. The dimensionless gas rise velocity was kept as for the symmetric Taylor bubble case $C_1 = 0.35$. Hence, a further decrease in the distribution parameter K is needed to account for that the gas will tend to move faster upwards than for the symmetric Taylor bubble case. Here one can also note that we only calibrated K for the situation where the Taylor bubble became stagnant. As we see from the comparison with the experiments, the error between simulated gas velocity and experimental gas velocities becomes larger than zero when the downward rate is increased above the critical rate. This indicates that the K value changes from the situation where the Taylor bubble is stagnant in the pipe to the situation where the Taylor bubble moves downwards.

Much later, one started to investigate under which conditions the Taylor bubble could become asymmetric. In Lu and Prosperetti [25], a mathematical stability analysis was performed where the effects of surface tension and viscosity were neglected. They derived a criterion for when the Taylor bubble would lose its symmetry. In our notation, this should occur if the downward bullheading rate exceeds $Q_1 = 0.135A\sqrt{gD}$. In our case, this would give $Q_1 = 0.10l/s$. We observed the phenomena for a larger rate than this so the criteria fits in our case in the sense that the instability should have occurred.

Later in Figueroa-Espinoza and Fabre [18] and [26] , the transition from symmetric to asymmetric shape of the Taylor bubble was studied further using both simulations and experiments. In the experiments [18], they considered vertical pipes with diameters 0.02, 0.04, and 0.08 meters. The fluids considered were water and water-glycerol mixtures. In their work, the effect of surface tension was considered when a transition criterion was developed. In our notation, the transition will occur if the bullheading rate Q satisfies the inequality (Q positive):

$$\frac{4Q}{A\sqrt{gD}} > (\frac{30}{Eo} + 0.06) \pm 0.07 \tag{10}$$

Hence, if the bullheading rate exceeds $Q_2 = [0.025, 0.051]$l/s, Taylor bubbles can lose the symmetry. For the rates used in our experiment, this condition was fulfilled for all rates considered. However, in future works it would be interesting to study a wider range of flowrates to check the transition criteria in more detail and for which situations the transition occurs. We would also like to mention that there has been a very recent experimental study reported in Kren et al. [27]. They also presented a detailed literature review.

In more recent years, one has seen a shifted focus to study more viscous systems and more extended use of Computational Fluid Dynamics (CFD) to study Taylor bubble movement in vertical and inclined flow. Here different sets of simulations are performed based on specific ranges for the dimensionless numbers discussed above. In Lizarraga-Garcia et al. [19], they investigated seven combinations with $\mathrm{Eo} \in [10, 700]$ and $\mathrm{Mo} \in [1 \times 10^{-6}, 5 \times 10^{3}]$. This was motivated from typical oil properties. They studied both upward and downward flow of liquid for both vertical and inclined configurations. In a few cases, the Taylor bubble also moved downwards. From the CFD simulations, they predicted the C_0 parameters. They also tested the criteria for transition from symmetric to non-symmetric Taylor bubbles discussed above. They indicated that viscosity may also play a role in this transition.

In Liu et al.[21], Taylor bubbles in vertical and inclined annular geometries were studied and CFD simulations were performed for $\mathrm{Eo} \in [40, 300]$, $N_f \in [40, 320]$ using various bullheading rates. The inverse viscosity numbers were chosen to reflect more viscous flow systems. In the CFD simulations, they also observed that bubble tip would move towards the outer wall as the counter current flow increased.

Based on the generated data for the vertical case they proposed a correlation for the dimensionless gas rise velocity C_1 expressed as function of the dimensionless numbers. They also proposed a correlation for C_0. This tended to increase and stabilize at values above 1 for increasing Eo and N_f numbers. From our perspective, it does not seem to fit for our experimental results. But this might not be expected since different geometries are considered. However, the authors point out that there are limited published results regarding correlations for C_0 in vertical counter-current flow.

5 Conclusion

Predicting what flow rates are needed to push gas bubbles downward in wells is important both for well control purposes and for killing producing wells. However, at the current stage, the gas slip models are not properly developed to account for the abrupt shift in the distribution parameter when a Taylor bubble changes from a symmetric position to the situation where the Taylor bubble tip lends towards the outer pipe wall. This leads to an underestimation of the required bullheading rate if one adopts gas slip parameter values typically used for upward two-phase flow.

In our work, we observed that the distribution parameter K reduced from the recommended value of 1.12 to 0.7. This reduction turned out to be in accordance with experimental observations reported earlier in the literature. The effect is that the gas moves faster upwards than expected. Also, more recent CFD studies indicate that Taylor bubbles can become non-symmetric if the downward flow of liquid is sufficiently large.

There has been developed two criteria for when the transition for symmetric to non-symmetric Taylor bubbles will take place. This seemed to be fulfilled in our experimental case, but it was not studied in detail and a wider range of flowrates should have been considered to check the transition criteria more in detail.

In our work, we used a transient flow model in combination with the experiments to validate the calibrated distribution parameter. We found it useful to combine this for demonstration purposes but also for gaining more insight into the flow dynamics.

There is a need for developing better models for how the distribution parameter will change in certain counter-current flow situations. Here, one should also consider that both more viscous Newtonian and non-Newtonian fluids systems are relevant. One must also consider both pipe and annular geometries covering both vertical and inclined cases since these represent the well geometries that one will experience in the field.

References

1. Oudeman, P., Avest, Dick ter, Grodal, E.O, Aasheim, H.A and Meissner, R.J.H. (1994), Bull Heading to Kill Live Gas Wells. SPE 28896. https://doi.org/10.2118/28896-MS
2. Bourgoyne, A.T and Koederitz, W.L. Gas Kick Behaviour During Bullheading Operations. https://www.bsee.gov/sites/bsee.gov/files/tap-technical-assessment-program//008cd.pdf. 1995. Last accessed 9 Jan 2024
3. Bourgoyne, A.T., Koederitz, W.L. and Bacca, H. 2001. An experimental study of bullheading operations for control of underground blowouts. https://www.bsee.gov/sites/bsee.gov/files/tap-technical-assessment-program//008dr.pdf. Last accessed 9 Jan 2024
4. Ben Gedge, Harpreet Kaur Dalgit Singh, Elsofron Refugio, Bao Ta Quoc, Nguyen Viet Bot. 2013. Managed Pressure Drilling – A Solution for Drilling the Challenging and Un-Drillable Wells in Vietnam and South East Asia. SPE 165775. https://doi.org/10.2118/165775-MS
5. M Noreffendy Jayah, Intan Azian A Aziz, Travis Mathews, Allan Voshall. 2013. Implementation of PMCD to Explore Carbonate Reservoirs from Semi-Submersible Rigs in Malaysia results in Safe and Economical Drilling Operations. SPE 163479. https://doi.org/10.2118/163479-MS
6. Alarcon, M.A.A and Hernandez, O. G. P.: Experimental Investigation and Transient Flow Modelling of the Bullheading Process. Master thesis. University of Stavanger. 2020. https://uis.brage.unit.no/uis-xmlui/handle/11250/2683701
7. Rabenjafimanantsoa, A.H., Jafarguluzade, J. and Time, R.W.: The rising of Taylor bubble at the inception to an annulus. In: Annual Transactions of the Nordic Rheology Society, Vol. 30, pp. 129-134. 2022. https://nrs.blob.core.windows.net/pdfs/nrspdf-c50305bc-4797-437f-b6cc-07d9a105738e.pdf
8. Pasco User Guide. https://www.pasco.com/

9. Abdelgadir, M.: Simulation Study and Modelling Improvements for the Bullheading Process. Master thesis. University of Stavanger. 2022. https://uis.brage.unit.no/uis-xmlui/handle/11250/3020289
10. Rasheed, F. and Ramstad, M.F.: An Experimental Investigation of the Bullheading Process with Newtonian Fluid in the Lab. Master thesis. University of Stavanger. 2024. https://uis.brage.unit.no/uis-xmlui/handle/11250/3152406
11. Ghauri, A.A., Fjelde, K.K. and Frøyen, J.: A Transient Model for Hydraulic Simulation of Bullheading and Pressurized Mud Cap Drilling. In: OMAE2016-54293 presented at the ASME 2016-35th International Conference on Ocean, Offshore and Artic Engineering. (2016) https://doi.org/10.1115/OMAE2016-54293
12. Benzoni-Gavage, S.: Analyse numérique des modèles hydrodynamiques d'écoulements diphasiques instationnaires dans le réseaux de production pétrolière. Thése. Université Claude Bernard Lyon I, ENS de Lyon, France. 1991
13. Zuber, N. and Findlay, J.A.: Average Volumetric Concentration in Two-Phase Flow Systems. J. Heat Transfer. 87(4): 453-468. 1965. https://doi.org/10.1115/1.3689137
14. Hasan, A.R., Kabir, C.S., Sayarpour, M.: A Basic Approach to Wellbore Two-Phase Flow Modeling. Paper presented at the SPE Annual Technical Conference and Exhibition, SPE 109868-MS. 2007. https://doi.org/10.2118/109868-MS
15. Evje, S. and Fjelde, K.K.: Hybrid Flux Splitting Schemes for a Two-Phase Flow Model. Journal of Computational Physics 175(2):674-701. 2002. https://doi.org/10.1006/jcph.2001.6962
16. Lorentzen, R. J. and Fjelde, K. K.: Use of Slopelimiter Techniques in Traditional Numerical methods for Multi-phase Flow in Pipelines and Wells. Int. J. Numer. Meth. Fluids 48 (7): 723–745. 2005. https://doi.org/10.1002/fld.952
17. Martin, C. S.: Vertically Downward Two-Phase Slug Flow. ASME. J. Fluids Eng. 98 (4):715-722. 1976. https://doi.org/10.1115/1.3448466
18. Fabre, J. and Figueroa-Espinoza, B.: Taylor bubble rising in a vertical pipe against laminar or turbulent downward flow: symmetric to asymmetric shape transition. Journal of Fluid Mechanics. 755: 485:502. 2014. https://doi.org/10.1017/jfm.2014.429
19. Lizarraga-Garcia, E., Buongiorno, J. and Al-Safran, E. Computational Fluid Dynamics (CFD) Simulations of Taylor Bubbles in Vertical and Inclined Pipes. SPE J. 26(06): 3832-3847. 2021. https://doi.org/10.2118/205373-PA
20. Liu, Y., Ozbayoglu, E.M., Upchurch, E.R. and and Baldino, S. Computational fluid dynamics of Taylor bubbles rising in vertical and inclined concentric annuli. International Journal of Multiphase Flow. 159. 2023. https://doi.org/10.1016/j.ijmultiphaseflow.2022.104333
21. Liu, Y., Mitchell, T., Upchurch, E.R., Ozbayoglu, E.M. and Baldino, S. Investigation of Taylor bubble dynamics in annular conduits with counter-current flow. International Journal of Multiphase Flow. 170. 2024. https://doi.org/j.ijmultiphaseflow.2023.104626
22. White, E.T. and Beardmore, R.H. The velocity of rise of single cylindrical air bubbles through liquids contained in vertical tubes. Chemical Engineering Science. 17(5): 351-361. 1962. https://doi.org/10.1016/0009-2509(62)80036-0
23. Griffith, P. and Wallis, G.B. Two-Phase Slug Flow. J. Heat Transfer. 83(3): 307-318. 1961. https://doi.org/10.1115/1.3682268
24. Nicklin, D.J., Wilkes, J.O. and Davidson, J.F. 1962. TWO-PHASE FLOW IN VERTICAL TUBES. TRANS. INSTN CHEM. ENGNR, Vol 40: 61:68.
25. Lu, X. and Prosperetti, A. Axial stability of Taylor bubbles. J. Fluid. Mech. 568: 173-192. 2006. https://doi.org/10.1017/S0022112006002205

26. Figueroa-Espinoza, B. and Fabre, J. Taylor bubble moving in a flowing liquid in vertical channel: transition from symmetric to asymmetric shape. J. Fluid Mech. 679: 432-454. 2011. https://doi.org/10.1017/jfm.2011.159
27. Kren, J., Zajec, B., Tiselj, I., Shawish, S.E., Perne, Z. and Tekavic, M. and Mikuz, B. 2023. Dynamics of Taylor bubble interface in vertical turbulent counter-current flow. International Journal of Multiphase Flow. 165. 2023. https://doi.org/10.1016/j.ijmultiphaseflow.2023.104482